MODELING AND CONTROL OF A STABILIZATION SYSTEM

KAMİL AFACAN

DECEMBER 2004

MODELING AND CONTROL OF A STABILIZATION SYSTEM

A THESIS SUBMITTED TO
THE GRADUATE SCHOOL OF NATURAL AND APPLIED SCIENCES
OF
MIDDLE EAST TECHNICAL UNIVERSITY

BY

KAMİL AFACAN

IN PARTIAL FULFILLMENT OF THE REQUIREMENTS
FOR
THE DEGREE OF MASTER OF SCIENCE
IN
MECHANICAL ENGINEERING

DECEMBER 2004

Approval of the Graduate School of Middle East Technical University

Prof. Dr. Canan ÖZGEN
Director

I certify that this thesis satisfies all the requirements as a thesis for the degree of Master of Science.

Prof. Dr. Kemal İDER
Head of Department

This is to certify that we have read this thesis and that in our opinion it is fully adequate, in scope and quality, as a thesis for the degree of Master of Science.

Prof. Dr. Bülent Emre PLATİN
Co-Supervisor

Prof. Dr. Tuna BALKAN
Supervisor

Examining Committee Members

Prof.Dr. Samim ÜNLÜSOY	(METU, ME)	_________________
Prof.Dr. Tuna BALKAN	(METU, ME)	_________________
Prof.Dr. Bülent Emre PLATİN	(METU, ME)	_________________
Prof.Dr. Mehmet ÇALIŞKAN	(METU, ME)	_________________
Burak GÜRCAN (M.Sc. in ME)	(ASELSAN)	_________________

I hereby declare that all information in this document has been obtained and presented in accordance with academic rules and ethical conduct. I also declare that, as required by these rules and conduct, I have fully cited and referenced all material and results that are not original to this work.

Name, Last name : Kamil AFACAN

Signature :

ABSTRACT

MODELING AND CONTROL OF A STABILIZATION SYSTEM

Afacan, Kamil
M.S., Department of Mechanical Engineering
Supervisor : Prof. Dr. Tuna Balkan
Co-Supervisor: Prof. Dr. Bülent Emre Platin

December 2004, 76 pages

Elevation axis model of a barrel stabilization system is constructed. The nonlinearities which are considered in the model are orifice flow characteristics, coulomb friction, hard-stop limits, kinematics of the system and unbalance on the barrel. A Simulink® model for the servo valve, actuation system and barrel is constructed. Servo valve identification is made via the actual test data. Compressibility of the hydraulic fluid is taken into consideration while modeling the actuation system. Friction model is simulated for different cases. Controller of the system is constructed by two PIDs, one for each of the velocity and the position loops. Velocity feed forward can reduce the time to make a quick move by the system. The disturbance is evaluated from a given road profile and disturbance feed forward is applied to the system.

Keywords : Barrel Stabilization, Servo Valve Model, Friction Model, Disturbance Feed Forward

ÖZ

BİR STABİLİZASYON SİSTEMİNİN MODELLENMESİ VE KONTROLU

Afacan, Kamil
Yüksek Lisans, Makine Mühendisliği Bölümü
Tez Yöneticisi : Prof. Dr. Tuna Balkan
Ortak Tez Yöneticisi : Prof. Dr. Bülent Emre Platin

Aralık 2004, 76 sayfa

Bir namlu stabilizasyon sisteminin irtifa eksen modeli yapılmıştır. Sistem modellenirken karşılaşılan ve modele dahil edilen nonlineer bileşenler şöyle sıralanabilir: Akış karakteristiği, Coulomb sürtünmesi, mekanik sınırlayıcılar, sistemin kinematik yapısı ve namlunun kütle merkezi kaçıklığı. Servo valfin, tahrik sisteminin ve namlunun modelleri Simulink® ortamında yapılmıştır. Servo valf geçek test bilgileri kullanılarak tanımlanmıştır. Tahrik sistemi modellenirken hidrolik akışkanın sıkıştırılabilirliği dikkate alınmıştır. Sürtünme modeli değişik durumlar için koşturulmuştur. Sistemin denetimi temel olarak 2 PID'den oluþmaktadýr. Biri konumu diðeri hýzý kontrol etmektedir. Sistemin ani hareket yapmasý için gereken zamaný azaltmak için hýz isteði ileri beslemesi yapýlmýþtýr. Bozucu sinyal belirlenen yol profilinden hesaplanmýþ ve bozucu sinyalin sisteme bildirimi gerçekleþtirilmiþtir.

Anahtar Kelime : Namlu Stabilizasyonu, Servo Valf Model, Sürtünme Modeli, Bozucu Ýleri Besleme

ACKNOWLEDGMENTS

The author wishes to express his deepest gratitude to his supervisor, Prof. Dr. Tuna Balkan and co-supervisor Prof. Dr. Bülent Emre Platin, for their guidance, advice, criticism and encouragement and insight throughout the research.

The author is also grateful to Prof. Dr. Kemal Özgören, Prof. Dr. Mehmet Çalışkan, Mr. Burak GÜRCAN and Asst. Kerem ALTUN for their suggestions and comments.

This study was supported by Turkish Naval Forces.

The author also would like to thank his wife Seda and his parents, for their encouragement and patience.

TABLE OF CONTENTS

LIST OF TABLES

LIST OF FIGURES

CHAPTER 1

INTRODUCTION

Weapons used in the battlefield are demanded to be lighter, more mobile, easily controllable and able to shoot with a high accuracy. One of these weapons used in land is the Main Battle Tank (MBT). MBT is probably the most important weapon because of its being mobile, armored and having heavy-fire capacity. Developments of MBT are parallel to the improvements in heavy weaponry, Weapon Control Systems (WCS) and hull mobility. Heavy weapons have became more effective with the improvements in material science and chemistry. Mounting of these weapons to the hull produces some problems. Control systems become more important while the system become larger and more complex. Drive technology and control systems determine the size of the MBT. Hull mobility depends on the vehicle technology to overcome the problems of cross-country movement.

Mobility demands in battlefield lead to the requirement of firing while moving instead of stopping at each time the MBT engages a target. This demand can be achieved by WCS by minimizing the tank's hull movement effects on the barrel.

In early tanks used in World War I, free elevation type of mounting was used and it was controlled by a shoulder strap. As the weapons got heavier this control became impossible and changed with manually operated gears. Up to 1940's this situation continued. The disadvantages of this setup are the insufficiently precise control, more human power and very low speed while steering the barrel. This is followed by the use of hydraulic drive systems. After electrical motors were used for slewing the barrel, rapid and precise control has been satisfied. Improvements in traversing the turret were applied to the powered control of the elevation control of tank guns. This adoption has led to the stabilization of the barrel [1].

1.1 Stabilization of Barrel on a Main Battle Tank

Motion of vehicles causes some unwanted movements on the barrel. These movements must be minimized in order to hit a target while moving. Gunners are expected to minimize this effect especially in elevation by rotating the barrel in the opposite direction of the hull's motion. But the frequency of this kind of motion varies from 0 to 3-4 Hz while the response of the human operators is not more than 0.5 Hz [2].

In this situation, the effects of vehicle motion on the barrel can be minimized by stabilization systems which are designed to maintain the barrel position according to the earth. Figure 1 and Figure 2 illustrate the problem in detail [1].

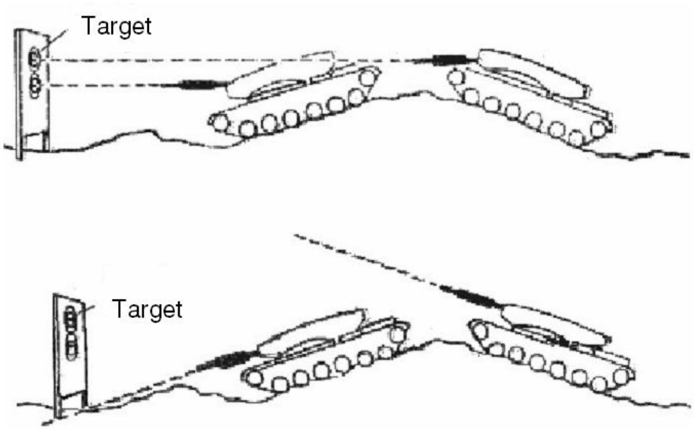

Figure 1. Barrel Motion with and without Stabilization System, in Elevation

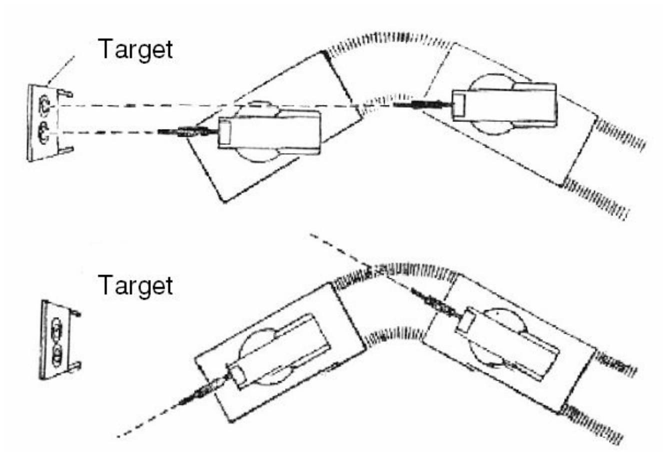

Figure 2. Barrel Motion with and without Stabilization System, in Azimuth

Systems aimed to do this stabilization basically closed loop servo systems which control the movement of the barrel relative to the earth by using gyroscopes and feedback signals produced by them.

Simplest stabilization systems are assigned to cope with the elevation changes and made up of a single closed loop system with a rate gyroscope mounted on the barrel to sense its angular velocity.

The "*basic systems*" involve two closed-loop servo systems, one for the elevation and the other for the azimuth axis of the gun. Each loop contains a gyroscope to sense the velocities in respective axis (Figure 3). Any difference between the sensed and the commanded velocities by the operator, cause to start the servo motors to nullify the error, hence to stabilize the turret. This type of two axes stabilization systems were developed during World War II.

Two axis control systems are proved to be effective, but it was not easy for the operators to correct the stabilization errors and the systems were not rapid enough to reduce the pointing errors to a sufficiently low level while the tank moves on a rough terrain.

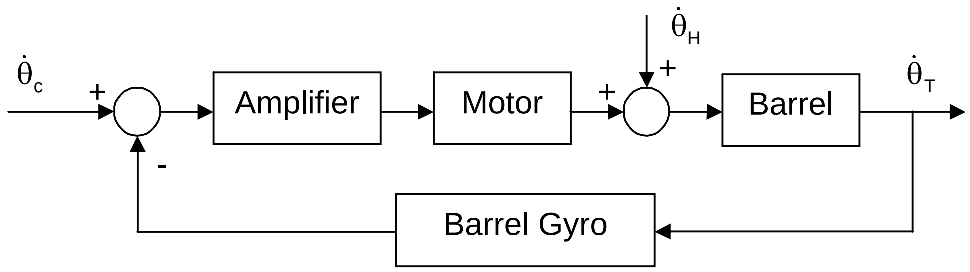

Figure 3. Closed Loop Servo for Basic System for one axis [2]

This led to the "*second-generation*" control systems in early sixties. These systems contain two extra gyros which feed the tank's movement forward in the system to make the turret more sensitive and rapid against the tank's movement (Figure 4). This method improved the stabilization of the guns. Second generation lowers the error by 50 % of the error in basic systems [3].

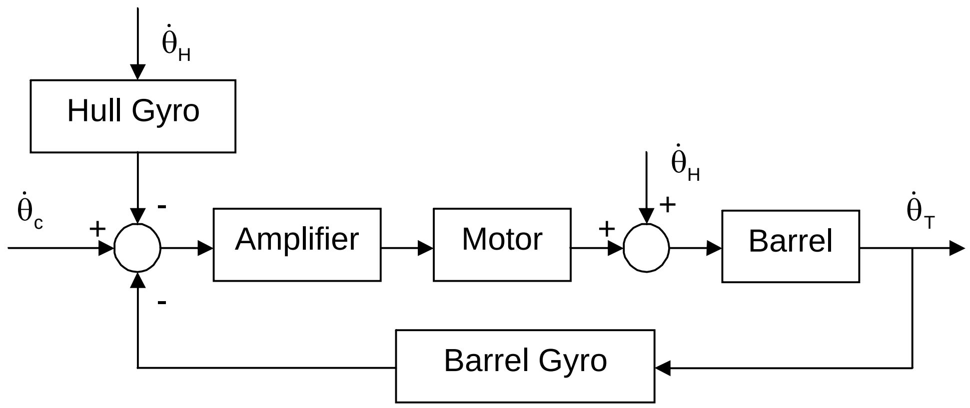

Figure 4. Second Generation Stabilization System for one axis [2]

To provide appropriate feed forward signals two gyroscopes are mounted one to the hull and the other to the barrel. The use of the feed forward control was pioneered by the Cadillac Cage Company in the late 1950s. This stabilization system was demonstrated in 1962 and firstly adopted to the Leopard I Tanks in 1969-1970 by German and Belgian Armies. Feed forward control application was seen in Soviet Army with a difference from the others. The stabilization systems include rate integrating gyros which provide a memory for the barrel position. So the barrel can be driven to the old position just before the disturbance.

"Director-type" system based on the independently stabilized gunner's sight was first developed in 1960s by the Delco Electronic Divisions of General Motors. Chrysler version of this system stabilized position of the gun only in elevation. A simpler alternative to this system was developed by Bofors Aerotronics in Sweden and by Marconi Command and Control Systems in England in the form of a pseudo-director system. The advantage of this system is that it provides a highly stabilized aiming mark without the complexity of an independently stabilized sight and can be applied readily to existing tanks with simple telescopic or periscopic sights mechanically linked to tank guns. In fact, Bofors Aerotronics produced this system, from 1983 onwards, for Centurion tanks. But it does nothing to improve the stability of the image which the gunner sees.

Another refinement is the introduction of rate-aided tracking. This represents an advance on the compensation of the angular motion of tanks. Although a rate-aided tracking is added, the gunner has to compensate for any changes in motion of the target [2,3]. Nevertheless, it improves the performance. Delco Electronics produced and used this in Leopard 2, which became the first tank to go into service.

Hence the barrel stabilization is mostly related to military and defense and it is treated as classified and therefore its details are not available in open literature. Some of the studies about this subject can be listed as follows.

In 1984, Balaman is studied the control of a manipulator with two angular degrees of freedom. This study is dealed with modeling and optimization of the system. It does not include the friction [4].

In 1998, Purdy enhanced the stabilization ratio by using the hull rate gyroscope for feed forward. This study gave the results of the simulations of linear and nonlinear model with and without disturbance feed forward and nonlinear model with feed forward and friction compensation [5]. In another study in 1999, Purdy made a simple elevation model and examined the out of balance effect on WCS [6]. These studies deal about the electrical drive technology. They also have no model in a computer program revealed in the publications.

A stabilization and hull model is developed by Şahin in 2001. In this study all the system elements were assumed to be linear. Stabilization was tried to be satisfied with the controller. There was no disturbance feed forward to stabilize the system [1].

1.2 Aims of the Study

In this study, the stabilization of the barrel on a MBT in elevation axis is considered. Only the elevation axis is considered because it is affected much more than the azimuth axis from the road profile. Since a stabilization system improve an ability of hitting targets while the tank is moving without stopping, the effects of disturbances on the barrel should be taken into account.

Unbalance caused by mounting the barrel off center of mass, friction at joint, hydraulic actuator as the driving unit and control system are the causes of using a stabilization system. In this study, all of these components are modeled and simulated under specified conditions.

The brain of the stabilization system is the controller. PID controllers are used to control the position and the velocity of the system. To be able to tune the parameters of the controller, either an experimental setup should be used or a model should be constructed. The use of experimental setup may cause trouble and may be dangerous for the setup. To prevent from these undesired situations such as damaging the system elements, operator injury etc., a model will be constructed and controller parameter tuning and system modifications will be realized by using this model.

Finally, the whole system or the elements of it can be used for other design and modernization studies.

1.3 Scope of the Study

It is intended in the study to model the elevation axis of a barrel completely in Simulink® 5.0 in Matlab® 6.5 environment and simulate the disturbance effects on it. This model includes barrel, hydraulic actuator as driving unit, an electro-hydraulic servo valve to manipulate the actuator and a controller unit.

In Chapter 2, the system elements are modeled and assumptions made while modeling are noticed for every element.

The properties of the servo valve used to control flow are explained. A system identification is made for the servo valve by using its experimental test outputs to determine the valve gain and the time constant. The nonlinear flow characteristics of the servo valve are derived and modeled.

The actuation system as a slider-crank mechanism is modeled. Inverse kinematics is used to solve the relation between the barrel's angular position and the actuator position while the motion is transformed from translational movement to rotational.

There are a lot of parameters which define the barrel's motion such as frictions in the barrel joint, the compressibility of the hydraulic fluid, unbalance caused from mounting point of the barrel to the hull and inertia.

The controller is made up of two PID's one for each loop feeding back the velocity and the position of the barrel.

In Chapter 3, some possible stabilization strategies are discussed. The disturbance caused by the road and transferred over the hull is modeled. The stabilization method to overcome the disturbance which can be measured by means of gyroscopes is examined.

Two tests with fixed velocity at 20 km/h and 40 km/h are realized for an assumed road profile. Parameters and results are introduced in Chapter 4.

Finally, Chapter 5 discusses about the results and conclusions of the study.

CHAPTER 2

SYSTEM MODELING

Modeling is the starting point of design, production, test and control. A good modeling will settle most of the problems in the design step. Also in the production case, modeling will help to define many of the criteria. The test and control stages are also critical. Because of many restrictions, the control and the test stages are realized in a tight manner. On the other hand with a well designed model, tests can be made on the model without any damage risk to the system. All critical values can be tested and determined in this way. This will also give a chance to determine the limits of the system approximately proportional to the accuracy of the model. It can be helpful to select the controller parameters for the system. In all of these cases, the model shows its effect on the situation.

While modeling, it should not be forgotten that the more the properties introduced to the model the more the problems occur. If all the parameters of the real system were tried to be included in the model, this would probably generate many problems such as the increase in the number of the logical operators, time spent for the evaluation, solver errors caused by the time step and more computer capabilities need etc. All of the real world can not be modeled in the same way. Sometimes modeling so many details becomes harmful instead of being helpful as the system may not be settled with the desired accuracy because of the problems mentioned above. While modeling, critical case is to determine the modeling criteria and assumptions.

While constructing the elevation axis model, the following assumptions are made:

- There is a stable source of hydraulic fluid supply at constant pressure.
- Effects of hydraulic fluid inertia are negligible.
- Gage pressures are used.
- No temperature change exists.
- There is no leakage.

2.1. System Model

In this study, the *"system"* will represent the union of the servo valve, the actuator and the barrel as seen in Figure 5. Hull dynamics is not included in the system mentioned in this study. While it is assumed that road profile is known and correctly transformed via the gyroscopes on the hull, it is included in the system as disturbance representing the hull motion. As the hull dynamics is not modeled here, all the inputs to the elevation axis model are accepted as the outputs of the hull dynamics directly.

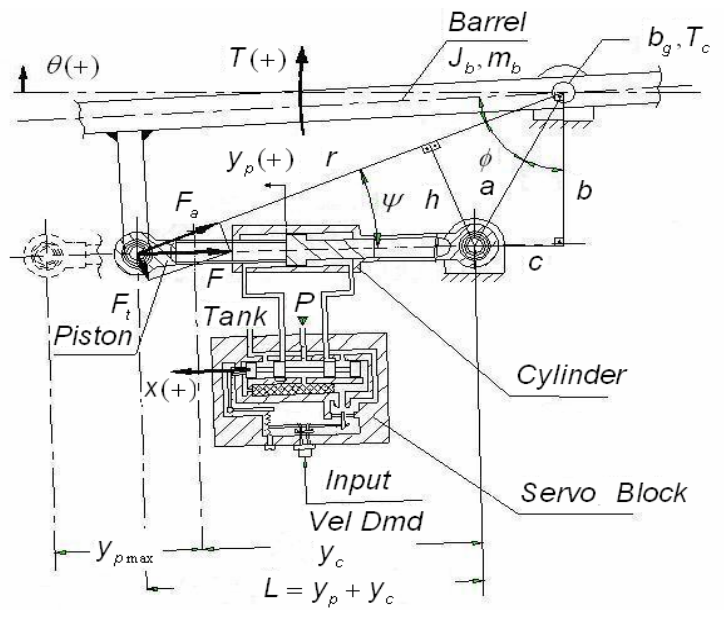

Figure 5. Schematic View of Valve, Actuator and Barrel (Adopted from [7])

The nomenclature used in Figure 5 is as follows.

T	:	Torque created by tangential force of the actuator component
J_b	:	Inertia of barrel
m_b	:	Barrel mass
x	:	Servo valve position
y_p	:	Stroke
y_c	:	Cylinder closed length
b_g	:	Viscous friction at barrel mounting
T_c	:	Static friction torque at barrel mounting
F	:	Force produced by actuator
F_t	:	Tangential force
θ	:	Angular position of barrel
P	:	Hydraulic fluid supply
L	:	Length of the stroke with cylinder closed length

Whole system is drawn as a block diagram in Figure 6.

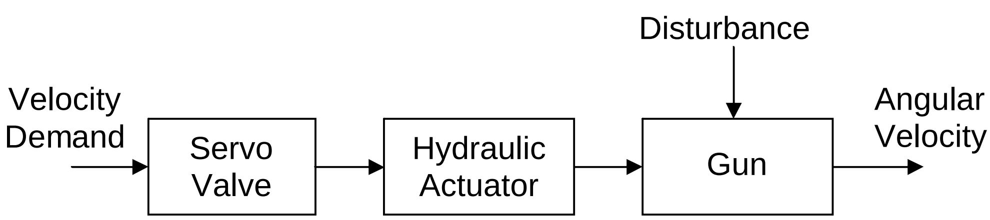

Figure 6. Block Diagram Representation of Barrel

Input of the system is the velocity command to the servo valve. The working fluid transports its energy to the actuator to be able to overcome the friction, move and stabilize the barrel at a demanded velocity with a desired accuracy.

2.2. Servo Valve Model

A classical four way, zero-lapped valve is used to excite the actuator. The servo valve has 3 stages; flapper as first, spools as second and third stages. A schematic representation of the valve used in this study is seen in Figure 7.

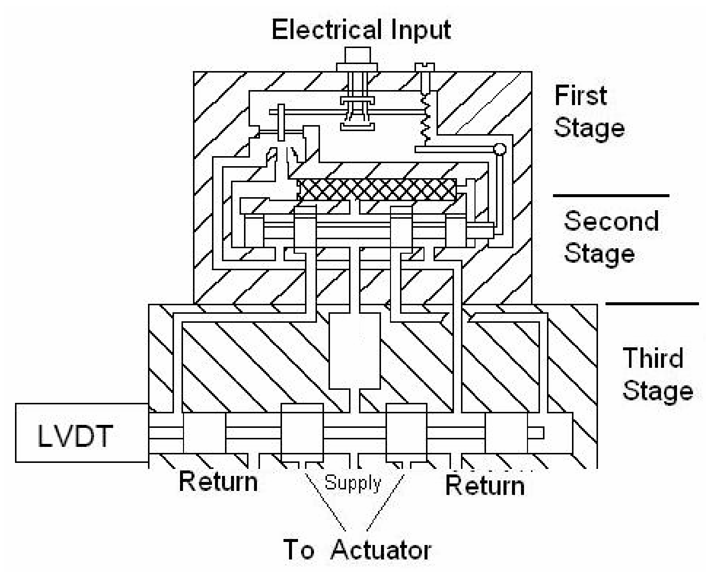

Figure 7. Schematic Representation of Servo Valve Block [7]

The first stage is an electrically driven flapper nozzle type. The flapper moves by the force generated from the induction of two coils by DC current. In the first stage the input is the current and the output is the flapper position. The flow characteristics is nonlinear but there is no chance to determine the position and the exact flow. By assuming that the force acting on the spool caused by the pressure in the chamber is proportional to the flapper position, it can be illustrated by a constant which will be the gain of the transfer function between the flapper and the spool position. In second stage, the input is the flapper position and the output is the spool position. In this case, also there is no chance to determine the position of the spool and the exact flow. At the third stage the position of the second stage spool is the input and third stage spool position is the output. Displacements and flows are indicated in Figure 8.

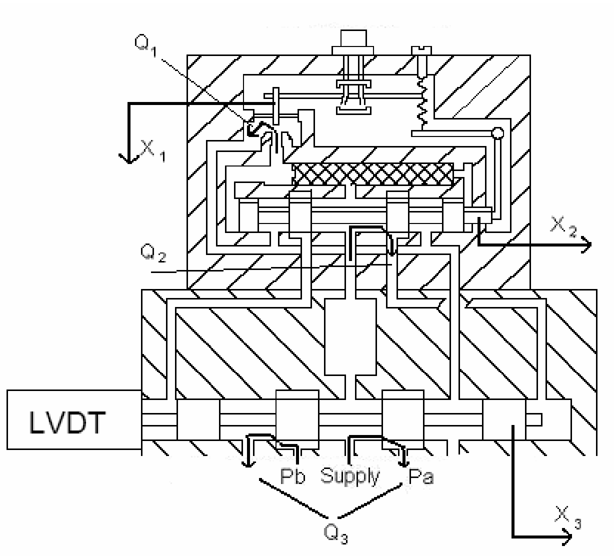

Figure 8. Displacement Axis and Flows in Servo Valve (Adopted from [7])

The block diagram of this servo valve will be as follows.

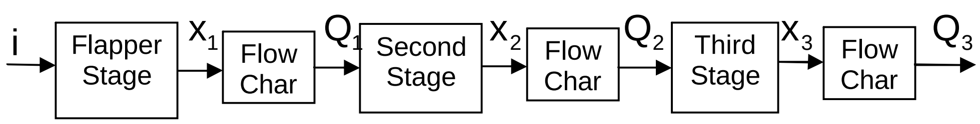

Figure 9. Three Stage Servo Valve Block Diagram

But a modeling servo valve as seen in Figure 9 is almost impossible while the parameters like mass, friction and stiffness of the stages separately are unknown. There is no chance to make individual tests for each stages of the valve. But, it is possible to determine the overall characteristics of the valve considering all three stages together. In these tests realized in ASELSAN just Linear Variable Differential Transducer (LVDT) outputs can be measured and recorded. LVDT is a device which determines the position of the spool and produce electrical signal proportional to this position. Because of these difficulties, the model of the valve can be modified as seen in Figure 10.

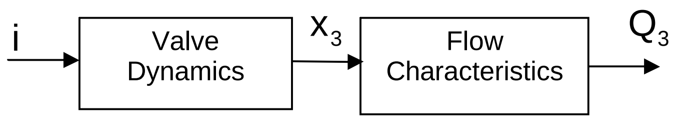

Figure 10. Servo Valve Illustration

In this block diagram, valve dynamics represents all three stages together. While the parameters of the electrical stages can not be evaluated, only the nonlinearity in the third stage is taken into account and the rest of the system is included in the transfer function of the plant. The output of the LVDT is measured and the flow rate is calculated from this value via orifice equation.

$$Q = C_d w x_3 \sqrt{\frac{2}{\rho}(p_1 - p_2)} \tag{2.1}$$

where;

Q : Volumetric flow rate

C_d : Orifice discharge coefficient

w	:	Width of the orifice inlet
ρ	:	Density of working fluid
p_1	:	Pressure at inlet of the orifice
p_2	:	Pressure at the exit of the orifice
x_3	:	The position of the third stage

For the dynamic characteristics of the valve, a second order transfer function can be used which represents a mass with friction. If this transfer function and (2.1) is substituted in Figure 10, block diagram of the servo valve can be drawn as shown in Figure 11.

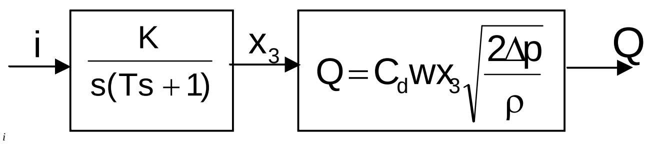

Figure 11. Block Diagram of the Servo Valve Model

Here are the assumptions made while modeling the servo valve.

- Temperature change in the fluid is neglected.
- Valve case is absolutely rigid.
- Compressibility of the hydraulic fluid is negligible because valve chambers are too small comparing to the volumes of the actuator chambers.
- Both spools are zero-lapped.
- There is no internal leakage in the valve.

2.2.1 System Identification

Computer simulations of systems give the opportunity to the users to study on the computer to make the design instead of constructing real systems. Thus less money and time will be spent for this job. While simulating these systems, all of the possible system parameters are tried to be illustrated in computer to determine a better starting point to the design case. But it should not be expected that the response of the simulations will be the same as the real system even parameters of the real system are known. On the other hand, there are a lot of systems for which the parameters can not be determined while there will be no chance to examine the elements of the system individually and measurement device capability and the accuracy will be effective. These kinds of system need to be identified.

Matlab® and similar programs introduce us many methods to identify the systems. System Identification Toolbox is one of these opportunities. But in this study, instead of using these methods in Matlab®, a cost function which is defined as follows, will be minimized for identifying the servo valve parameters.

$$J = \sum_{k=1}^{n} (y_m - y_t)^2 \quad ; \quad k=1,2,.....,n \qquad (2.2)$$

where;

J	:	Cost function
y_m	:	Model output
y_t	:	Test output
n	:	Number of the samples

Servo valve used in the elevation axis model is identified in [7] with MATLAB® System Identification Toolbox®. The servo valve was excited with a square wave which had a changing amplitude so that different magnitude step responses were obtained as seen in Figure 12.

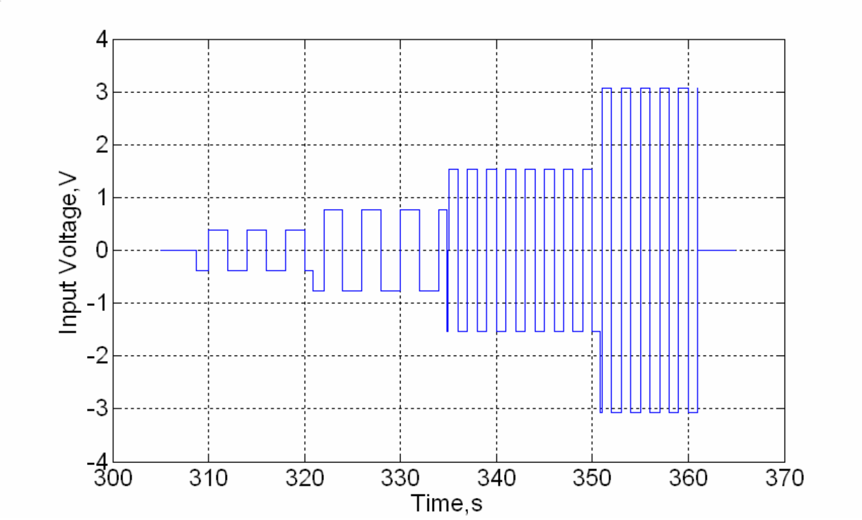

Figure 12. Input Signal of Servo Valve for System Identification [7]

The position of the spool was determined by a LVDT and recorded as the output. Making these tests at different amplitudes gave more information about the valve characteristics. The output plots can be seen in Figure 13. The valve was controlled by a PID while the position of the third stage spool (LVDT) is fed back [7].

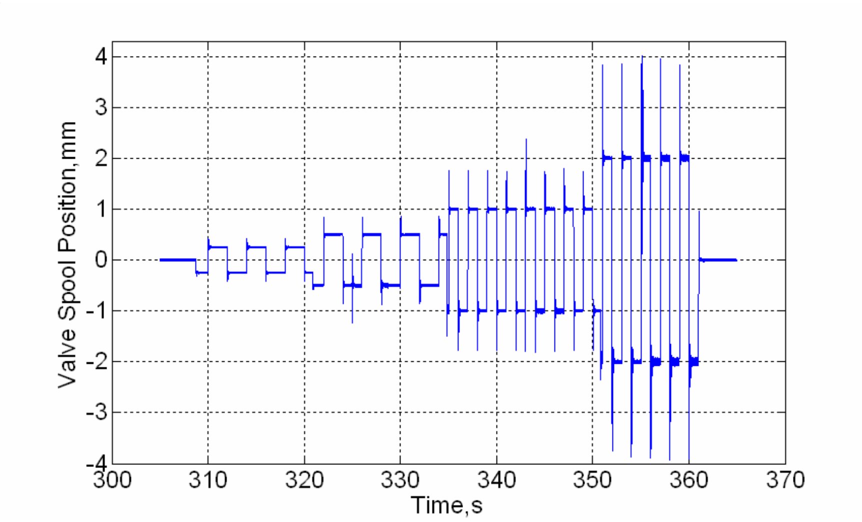

Figure 13. The LVDT Output of Servo Valve Test [7]

But this identification is made between the command input which is an electrical signal and the position of the valve in mm. In this study, this identification is repeated while taking the input as the position demand corresponding to the electrical input in mm.

As seen in Figure 13 there are transition periods and some disturbances which can not be used in identification. By omitting the transient periods and extraordinary fluctuations, step responses are obtained and plotted on the same graph in Figure 14 for one second duration, which is an enough period for settling.

A valve model which has the transfer function seen in Figure 11 is constructed. In this model, two parameters are tried to be determined, time constant,T of the valve and the valve gain,K. The time step is taken same as the test environment and sampling rate of the output data, $1x10^{-3}$ sec. These two parameters are determined via an “m” file with direct search method and cost function values are recorded in an error matrix.

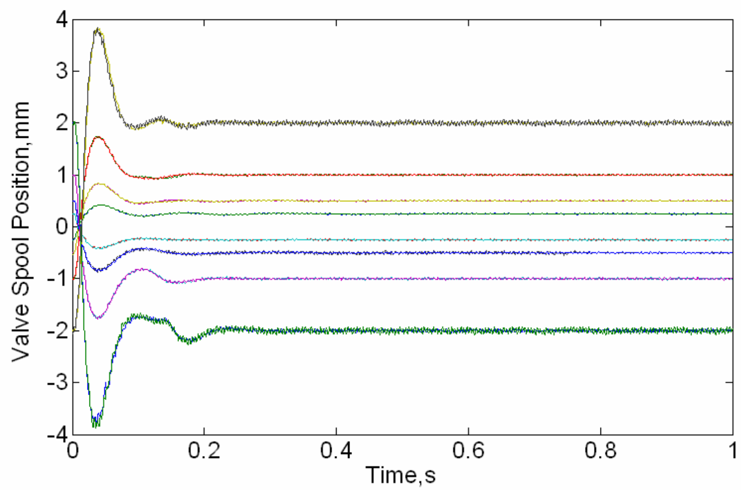

Figure 14. Servo Valve Spool Step Responses for Different Input Values

As can be seen in Figure 14, valve step responses differ from each other. Valve shows different dynamic behaviors at different amplitudes. In this situation, although identification will fit exactly to one of the step response, it would not be the optimum solution for the other magnitudes. Thus, the solution differs also at each amplitude. Anyone of the valve gain and time constant pairs for these step responses could not represent all of the step responses with the same accuracy. “m” files used in the simulations and calculation is given in Appendix 1.

Until now, the transfer function between the position command and the spool position is determined. The nonlinearity in the valve is maintained by using the orifice equation (2.1) to derive the flow from the valve.

2.2.2 Load Pressure Feedback

The servo valve is used to control the velocity of the actuator. Pressure feedback is a way of adding damping to this subsystem. Pressure feedback is able to increase damping based on the fact that the cylinder pressure is related to the derivative of the cylinder velocity. Feeding back the derivative of the cylinder velocity increases the damping of the system, thus improves the transient performance. The only problem with this strategy is that the pressure information also contains the effect of external forces. A high-pass pressure filter is introduced to deal with this problem. The form of the compensator is shown in equation (2.3) [8].

$$G_{HP} = \frac{\tau s}{\tau s + 1} \tag{2.3}$$

The τ value can be set through a wide range. Mostly, this parameter is selected for each specific system application separately and influenced by various system requirements such as system frequency, response and stiffness. τ generally corresponds to a corner frequency of about 1/3 of resonant load frequency, f_c [9].

$$\tau = \frac{1}{2\pi(f_c/3)} \tag{2.4}$$

Vibration tests were made for MBT to determine the critical frequencies. For the MBT the tests are made in a project in ASELSAN. Barrel's natural frequency is determined in these tests as 10.73 Hz [10].

2.2.3 Dither Signal

Behavior of a hydraulic servo valve can be unpredictable because of stiction which keeps the valve spool from moving when input signal changes are small. When the signal finally becomes large enough to initiate a movement, the spool will tend to overshoot the position required for accurate control. Dither is a rapid, small movement of the spool around the desired position. It is intended to keep the spool moving to avoid stiction. Dither amplitude must be large enough and the frequency slow enough for the spool to respond, and yet small and fast enough to avoid creating a noticeable pulsation in the hydraulic output of the valve. The amplitude of the ripples determines whether, or how far, the spool will move at a given frequency [11,12].

The dither signal can be applied to the system by adding this signal to the control command. It is usually about 25-300 Hz and magnitude is the 10 % of the reference control signal. In addition to this property, the dither signal prevents the contamination near the orifices inlets which work very little openings [13]. Command signal used in the system is 10 V for the full opening of the servo valve. The 10 % of this value corresponds to the peak-to-peak value of the amplitude of the dither signal. Dither signal used in this model is a sine wave with an amplitude 0.5 V at 140 Hz. These parameters are found in [7] and give the best performance without oscillation.

2.3. Actuator Model

Hydraulic actuator used in the system in this study is a double acting type as shown in Figure 15. The flow from the valve fills the actuator and pressurizes one side of the cylinder. Force required for the motion is produced by this pressurized liquid acting on the piston.

Actuator motion, fluid compressibility, actuator stiffness and the leakage in the actuator define the flow rate directly.

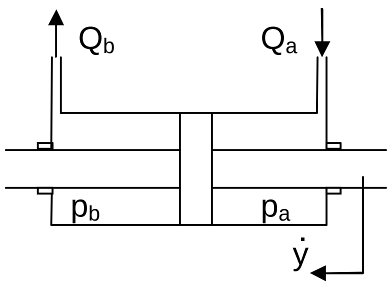

Figure 15. Double Acting Type Actuator

Finally the assumptions made while modeling the actuator is as follows.

- Temperature change in the fluid is neglected.
- Cylinder and pressurized lines are absolutely rigid.
- Piston mass is negligible.(Because barrel mass is too large)
- There is no internal leakage in the actuator.
- Compressibility is taken into consideration while volumes in the cylinder and its lines are too big compare to the servo valve.

Bulk modulus, β_e, is the measure of the compressibility of a fluid, defined as;

$$\beta_e = -V\frac{dp}{dV} \tag{2.5}$$

representing the stiffness of a hydraulic system. As the bulk modulus becomes bigger, the fluid becomes stiffer.

The compressibility is taken into consideration only while modeling the actuator because volumes in the actuator and pressurized lines are too large than the volumes in the servo valve.

While it is assumed that leakage flow is zero and the cylinder is absolutely rigid, equation for the conservation of mass can be written as in the following form for the chambers (2.6a and b) [14].

$$Q_a = A_a\dot{y} + \frac{v_a}{\beta_e}\dot{p}_a \tag{2.6a}$$

$$Q_b = A_b\dot{y} - \frac{v_b}{\beta_e}\dot{p}_b \tag{2.6b}$$

where;

Q_a : Flow rate into the cylinder's chamber a

Q_b : Flow rate out of the cylinder's chamber b

A_a, A_b : Net piston areas (rod area subtracted)

v_a v_b : Volumes of cylinder chambers

$\dot{p}_a$ $\dot{p}_b$: Time rates of changes in pressure in cylinder chambers

The causality relation between the flow rate, velocity of piston and the pressure can be explained as in Figure 16.

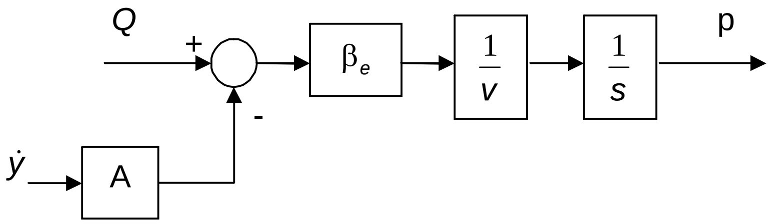

Figure 16. Causality Block Diagram of Flow Rate and Pressure

The net force produced in an actuator is the difference of the pressure forces at two sides of the piston.

$$F = p_a A_a - p_b A_b \tag{2.7}$$

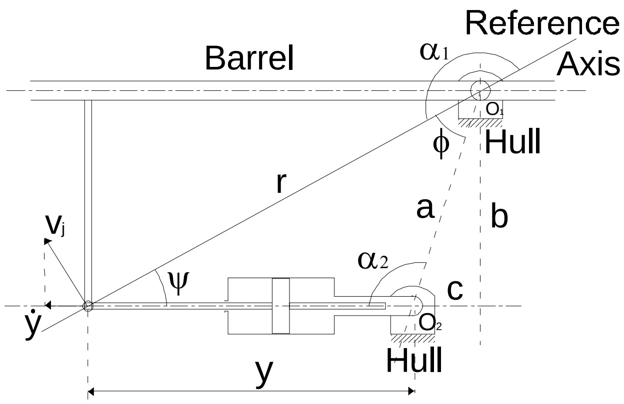

Figure 17. Barrel and Actuation (Slider Crank) Mechanism

The actuating system is a slider-crank mechanism in the system. The cylinder is fixed to the hull and the piston is mounted to the barrel like in Figure 17.

The output of the system is the barrel's angular position; input is the desired angular position of the barrel relative to the hull. On the other hand slider-crank has a translational input and a rotational output.

The unknown parameter which is the variable edge of the triangle for this mechanism is the length of the actuator. The loop closure equations are;

$$y\cos\alpha_2 = r\cos\alpha_1 + a \tag{2.8}$$

$$y\sin\alpha_2 = r\sin\alpha_1 \tag{2.9}$$

Solving the equations for α_1 and α_2;

$$\alpha_1 = \cos^{-1}\left(\frac{y^2 - r^2 - a^2}{2ar}\right) \tag{2.10}$$

$$\alpha_2 = \cos^{-1}\left(\frac{y^2 + a^2 - r^2}{2ay}\right) \tag{2.11}$$

Substituting (2.10) and (2.11) in definition of $\psi = \alpha_1 - \alpha_2$;

$$\psi = \cos^{-1}\left(\frac{y^2 - a^2 - r^2}{2ay}\right) - \cos^{-1}\left(\frac{y^2 + a^2 - r^2}{2ay}\right) \tag{2.12}$$

where;

y	:	Total length of piston and the cylinder
r	:	Radius of the rotation of barrel around the mounting to the hull
a	:	Length of the line connecting the mountings of the barrel and the cylinder to the hull
α_1	:	Angle between the reference axis and the r
α_2	:	Angle between the reference axis and the y
ψ	:	Angle between y and r

The relation between the rotational and the translational movement can be shown as follows.

$$V_j = \omega r \qquad (2.13)$$

$$\dot{y} = V_j \sin\psi \qquad (2.14)$$

where;

V_j : Tangential velocity of the piston about the instantaneous center of rotation

ω : Angular velocity of the barrel

r : Radius of the instantaneous center of rotation

Combining these two equations, gives

$$\dot{y} = \omega r \sin\psi \qquad (2.15)$$

2.4. Barrel Model

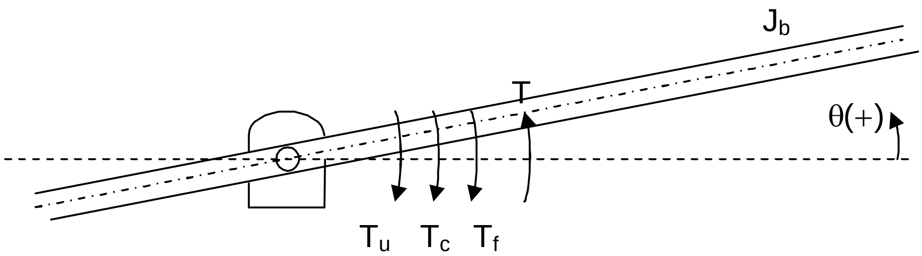

Figure 18. Torques acting on the Barrel

Referring to Figure 18 the equation of motion can be written as for the barrel.

$$J_b\ddot{\theta} = T - T_f - T_u - T_c \qquad (2.16)$$

where;

T	:	Torque applied to the barrel by the actuator
J_b	:	Mass moment of inertia of barrel
θ	:	Angular position of barrel
T_f	:	Viscous friction torque
T_c	:	Static friction torque
T_u	:	Unbalance torque

There are two hard-stops which limit the rotation of the barrel with respect to the hull at +20^o and -10^o. Hence these limits are relative to the hull. Also the joint between the barrel and the hull is not located at the center of gravity of the barrel and has both Coulomb and viscous friction. Geometrical structure of the actuation system, frictions and unbalance cause nonlinearity. In addition to the general assumptions, the barrel is assumed to be absolutely rigid.

A classical *"Coulomb + viscous friction"* characteristic can be shown as seen in Figure 19 [15].

While modeling, causality must be carefully followed. To be able to start the motion, static friction, T_c, must be overcame. Thus, in determining the situation whether *"stick"* or *"move"*, coulomb friction will be the first check point.

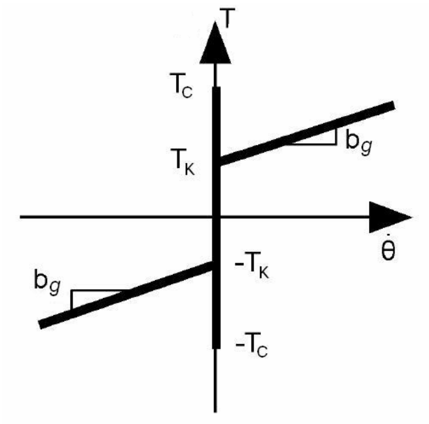

Figure 19. Coulomb + Viscous Friction Characteristics

The system is assumed to be stuck to the hull as the initial condition. Then the relative velocity will be zero and so will be the viscous friction. T_c^*, is the *"resultant torque"* of the actuation torque, unbalance torque and inertial torque. The resultant torque which tries to overcome the static friction torque can be defined as;

$$T_c^* = T - T_u - J_b\ddot{\theta}_T \tag{2.17}$$

where;

$\ddot{\theta}_T$: Angular acceleration of the turret

T_c^* : Resultant torque

Then, it is compared to the static friction torque. The barrel's status is defined with this comparison. The two possible results of this comparison can be shown as follows.

$$T_c \geq T_c^* \tag{2.18}$$

$$T_c < T_c^* \tag{2.19}$$

If the static friction is bigger than the resultant torque applied to the system, then the barrel will be stuck, otherwise barrel will move.

The other design criterion is the rotation limits of the barrel. It should not be forgotten that these limits are relative to the hull.

$$-10^{o} < \theta_R < +20^{o} \tag{2.20}$$

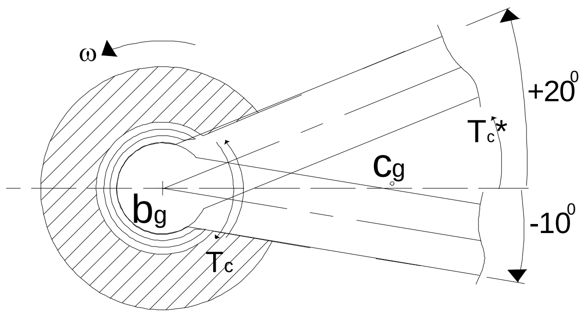

Figure 20.   Simplified View of the Barrel Joint

A simplified projection of the joint which mounts the barrel to the gun could help the problem to be understood better (Figure 20). In this case, outer part has an angular velocity and it is known. There is viscous friction, represented by b_g, and static friction, T_c between the outer and the inner part. Resultant torque, T_c^*, was defined before.

These comparisons are illustrated in the flow diagram in Figure 21.

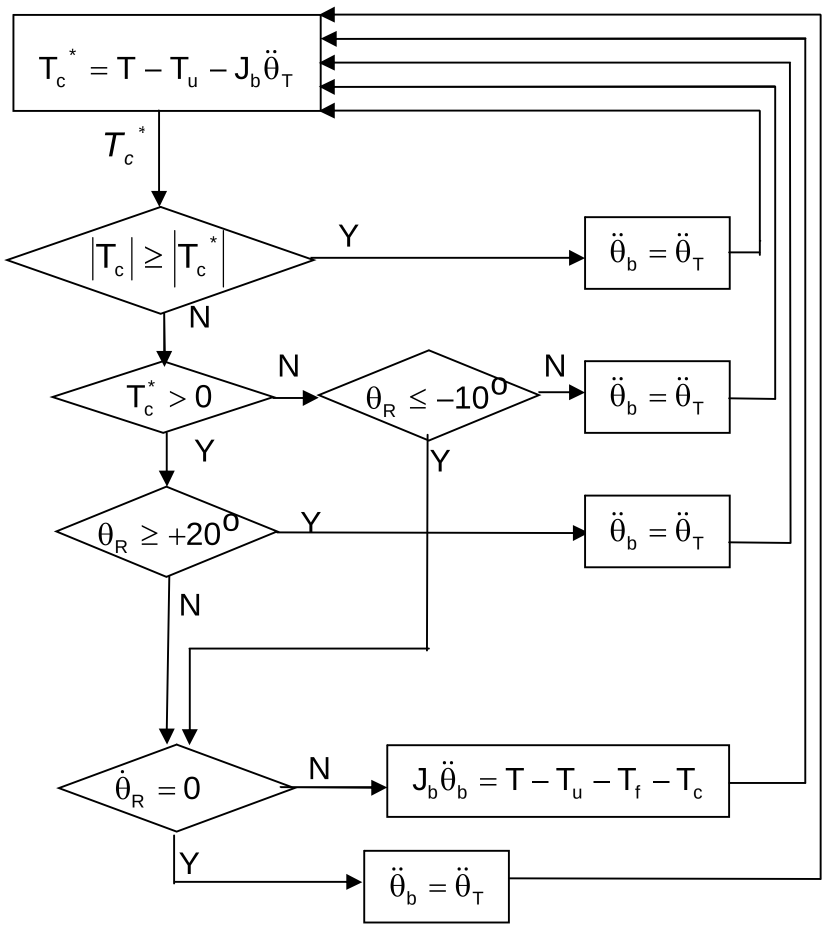

Figure 21. Flow Chart of Barrel Movement According to the Friction

Comparison of the friction torque and the resultant torque is made before to decide whether the motion starts or not. Since there are hard-stops, new comparisons should be made on the situation where the barrel is at limits in position.

While the barrel is at the negative limit, a resultant torque which is in the negative direction and naturally larger than the friction torque make no sense for the system. This torque tries to move the barrel beyond the limit and barrel is stuck in this situation. If the resultant torque is in the positive direction, barrel can move. On the other hand, when the barrel is at the positive limit, the direction effects on the system of the resultant torque are just the opposite of the first two cases. These are the conditions of passing from stuck to slip.

Another decision should be made about whether the barrel continues its motion or stops. Relative velocity and the position of the barrel are criteria for this case. Barrel sticks to the hull when any of the two conditions are satisfied. These two conditions are considered at the same time. One is the position check of the barrel whether it touches the hard-stops or not and the other is the velocity comparison of the inner part with the outer one.

2.4.1. Unbalance Effect

The unbalance is the result of the mounting the barrel to the hull from any where except its center of mass. Its effect on the barrel is an additional torque proportional to the displacement between the center of mass and the mounting and the angular position of the barrel with respect to the hull. The hull is assumed always parallel to the ground (Figure 22).

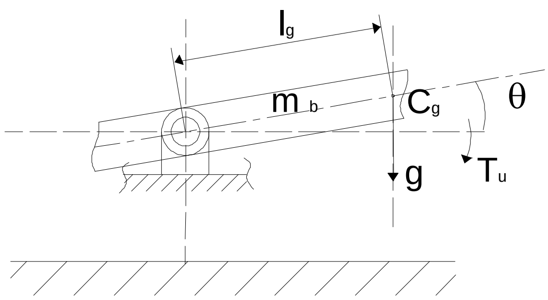

Figure 22. Unbalance Effect on the Barrel

The torque caused by the unbalance effect can be determined as follows.

$$T_u = m_b g l_g \cos\theta \tag{2.21}$$

where;

T_u : Unbalance torque

m_b : Mass of the barrel

l_g : Distance between the center of rotation and center of gravity

However, this is not the only factor which cause torque on the barrel in vertical axis. While the tank moves on a curved surface, it rotates around an instantaneous center of rotation of ground profile (Figure 23). This affects the barrel as disturbance which is an angular velocity. The rate of change of the angular velocity, α_d is the acceleration and causes torque in the system in the opposite direction with the angular velocity.

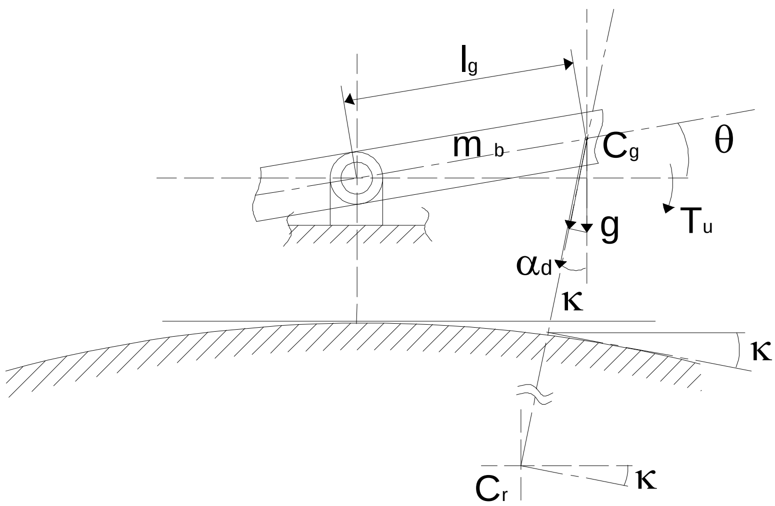

Figure 23. Instantaneous Center of Rotation and Normal Acceleration

By the addition of the normal acceleration to the system, the new unbalance torque equation can be rewritten as follows.

$$T_u = m_b(\alpha_d + g\cos\kappa)l_g \cos\theta \tag{2.22}$$

where;

α_d : Normal acceleration

κ : Angle between the tangent of the surface and the normal of the rotation axis

As mentioned before, road profile affects the barrel as the disturbance which is an angular velocity. The rotation is unique all over the tank around the instantaneous center rotation.

While the tank moves on a curve, S, with a constant speed of v, it goes Δs much in Δt time. While this motion, vertical displacement of the barrel is Δy much.

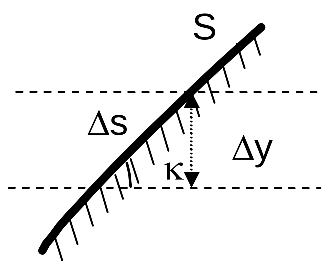

Figure 24. Angular Displacement on Road Profile

Angular displacement of the barrel is κ angle and angular velocity, demonstrated by ω, will be the change in κ angle. In this point of view, angular velocity, ω can be determined as follows.

$$\omega_d = \frac{d}{dt}\kappa \tag{2.23}$$

$$\Delta s = v\Delta t \tag{2.24}$$

$$\sin\kappa = \frac{\Delta y}{\Delta s} \tag{2.25}$$

Substituting (2.24) in (2.25) and (2.26) will give

$$\sin\kappa = \frac{\dot{y}}{v} \tag{2.26}$$

$$\kappa = \sin^{-1}\left(\frac{\dot{y}}{v}\right) \tag{2.27}$$

And from the definition of the angular velocity, it can be determined as

$$\omega_d = \frac{d}{dt}\left[\sin^{-1}\left(\frac{\dot{y}}{v}\right)\right] \tag{2.28}$$

Hence, the disturbance affecting on the barrel caused by the road profile is found.

CHAPTER 3

CONTROL STRATEGIES FOR DISTURBANCE REJECTION

Although different systems are designed to perform different functions, all of them have to meet some common requirements. Main characteristics of a typical system concern accuracy, speed of response and output sensitivity to component and environmental changes. The priority of importance of these characteristics is defined by the designer based on the system nature and its application. These characteristics are used to measure the performance of the system. But the primary concern is the stability of the system.

In this study, all of the criteria were tried to be satisfied but according to this specific application most important performance criteria is disturbance rejection in other words stabilization of the barrel in the elevation axis when the MBT moves on a bumpy road.

3.1. Controller

System has two outputs to be controlled namely the angular velocity and the position. Each loop, which are constructed by feeding back the system output to the comparison with the desired value, is controlled by a PID controller. The position and the velocities in the system are measured by different devices. The device used for measuring the velocity is a classical mechanical gyroscope both for the barrel and the hull. The position of the barrel is measured by an inclinometer. At first look, it seems meaningless but the feedback signals are supplied from different sources. The gyroscopes used in the system have a bandwidth of 30 Hz and a damping ratio of 0.7. Although they are relevant, in industrial applications controllers could be used in this way.

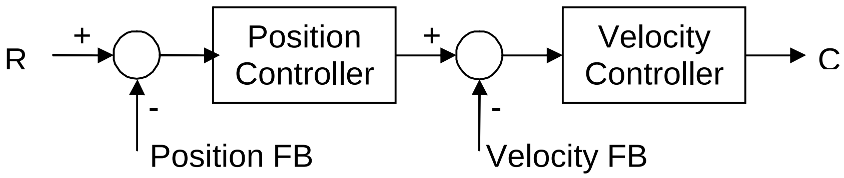

Figure 25. Classical Control Algorithm

Many parameters in the system and environment try to determine or affect the system output. System characteristics itself, while it has many nonlinearities, disturbances influence the controllers efficiency. Thus, some additional strategies may be used to eliminate these effects on the system to reject the disturbances more effectively.

3.2. Disturbance Feed Forward

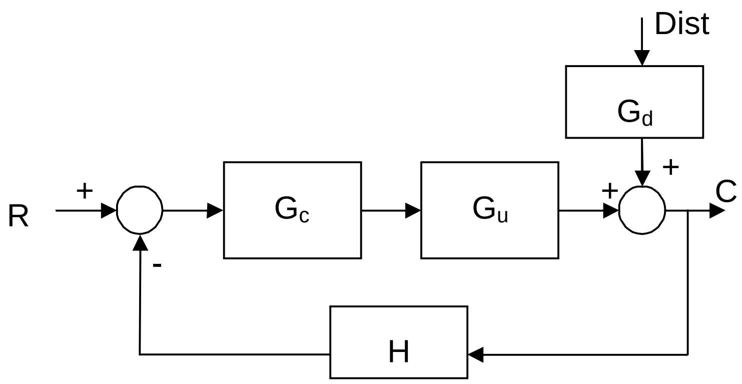

Figure 26. Feedback System with Disturbance Input

As the definition of disturbance, it is unwanted that adversely affect the desired output (Figure 26). Although the effect of disturbances on the system can not be eliminated completely, it can be reduced. To be able to improve the response, first of all disturbance must be determined [16].

To nullify the disturbance effects on the system, disturbance can be fed back to the input of the plant as seen in Figure 27.

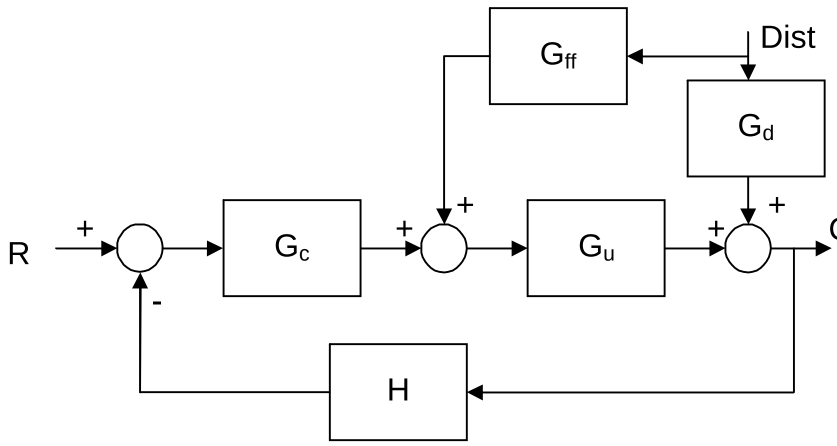

Figure 27. Feedback System with Disturbance Feed Forward

Ideally, the feed forward transfer function, G_{ff}, should be the inversion of the ratio of the disturbance transfer function and the nominal plant transfer function. It is not forgotten that the G_{ff} must be stable since it acts in open loop [17].

$$G_{ff} = -\frac{G_d}{G_u} \tag{3.1}$$

Frequency response of the system is analyzed to be able define the transfer function, G_u, between the command signal and the output.

Table 1 Frequency Response Data for G_d and G_u.

	Gd			**Gu**		
Frequency (Hz)	**20log M (dB)**	**Mag of input**	**Mag of output**	**20log M (dB)**	**Mag of input**	**Mag of output**
0.1	0.0054	0.2	0.2001	0.1998	0.2	0.1996
0.2	0.0506	0.2	0.2012	0.539	0.2	0.2128
0.3	0.055	0.2	0.2013	0.6656	0.2	0.2159
0.4	0.0796	0.2	0.2018	0.7432	0.2	0.2179
0.5	0.0867	0.2	0.202	0.8005	0.2	0.2193
0.6	0.0962	0.2	0.2022	0.8483	0.2	0.2205
0.7	0.1115	0.2	0.2026	0.8915	0.2	0.2216
0.8	0.1239	0.2	0.2029	0.9324	0.2	0.2227
0.9	0.1506	0.2	0.2035	0.9742	0.2	0.2237
1	0.1407	0.2	0.2033	1.016	0.2	0.2248
2	0.1729	0.2	0.204	1.5484	0.2	0.239
3	0.3445	0.2	0.2081	2.342	0.2	0.2619
4	0.5439	0.2	0.2129	3.3323	0.2	0.2935
5	0.6408	0.2	0.2153	4.4074	0.2	0.3322
6	0.9606	0.2	0.2234	5.2972	0.2	0.368
7	1.0884	0.2	0.2267	5.5959	0.2	0.3809
8	1.4413	0.2	0.2361	5.1497	0.2	0.3618
9	1.6767	0.2	0.2426	4.1001	0.2	0.3207
10	1.7434	0.2	0.2445	2.7229	0.2	0.2736
13	2.0475	0.2	0.2532	0.4917	0.2	0.2116
16	3.1989	0.2	0.2891	-1.0748	0.2	0.1767
20	7.1993	0.2	0.4581	-2.0245	0.2	0.1584
23	8.5271	0.2	0.5338	-0.9974	0.2	0.1783
26	13.6972	0.2	0.968	0.3915	0.2	0.2092
30	25.8101	0.2	3.9042	-0.1859	0.2	0.1958
33	11.3783	0.2	0.7412	-3.1657	0.2	0.1389
36	5.7344	0.2	0.387	-8.6341	0.2	0.074
40	4.6665	0.2	0.3422	-14.1794	0.2	0.0391
50	-2.0602	0.2	0.1578	-23.9876	0.2	0.0126
60	-5.9759	0.2	0.1005	-30.9814	0.2	0.0056
70	-8.6592	0.2	0.0738	-36.5776	0.2	0.003
80	-10.7546	0.2	0.058	-41.0167	0.2	0.0018
90	-12.6257	0.2	0.0467	-44.7575	0.2	0.0012
100	-14.0877	0.2	0.0395	-47.6867	0.2	0.0008

Identification of the disturbance transfer function, G_d, and the transfer function of the nominal plant are made by using the frequency response. This identification is made on the Simulink® model.

In tests, system is separated from the controller and naturally from the loops. System is used as open loop. Only servo valve position feedback, LVDT is closed. Coulomb friction is neglected. Both input command to the open loop system and disturbance are sine wave at an amplitude of 0.1 rad/s with different frequencies.

Angular velocity demand which is fed to the system model at different frequencies with an amplitude of 0.1 rad/s is checked whether it cause any saturation in the system or not. After recording the outputs Bode plot can be obtained.

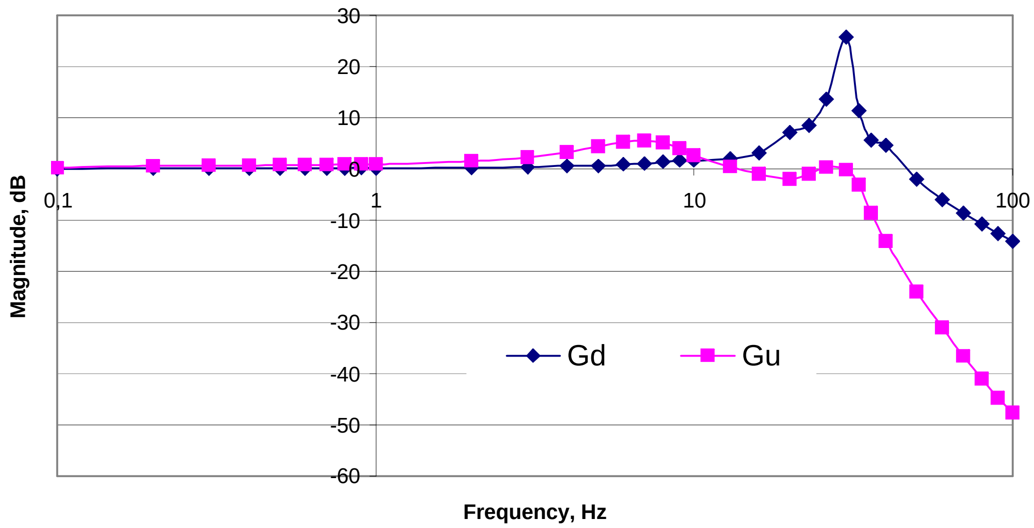

Figure 28. Bode Plot of Plant’s and Disturbance Transfer Functions

As seen from the figure, transfer functions have a low pass characteristics and it should be expected that the G_{ff} must have a high pass characteristic. Corner frequency can be easily determined from Figure 28 as 27 Hz or approximately 170 rad/s.

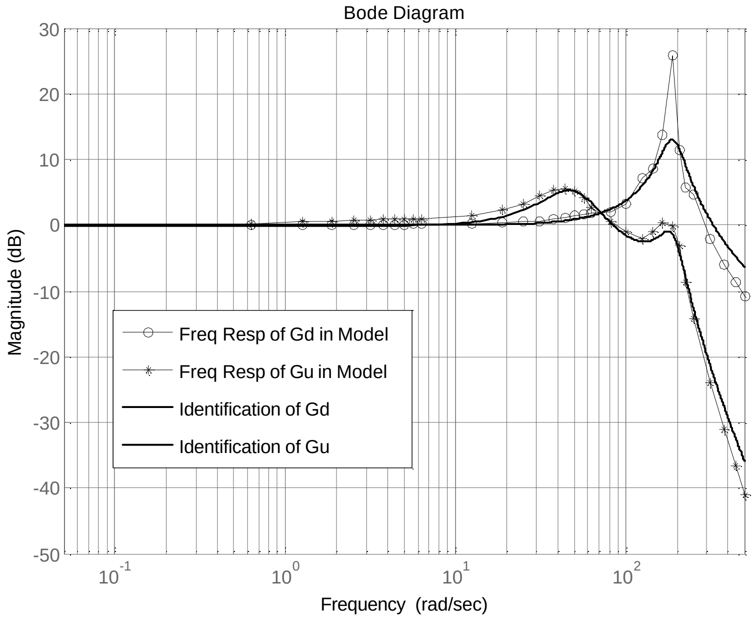

Figure 29. Bode Plot of the Disturbance and the Plant and the Identifications

At the end of the identification of G_d and G_u as seen in Figure 29, the transfer functions can be written as follows.

$$G_d = \frac{0.08469s^3 + 18.92s^2 + 796.8s + 36100}{0.0004s^4 + 0.04032s^3 + 16.41s^2 + 638.4s + 36100} \tag{3.2}$$

$$G_u = \frac{680s + 35360}{0.0004s^4 + 0.04032s^3 + 16.41s^2 + 638.4s + 36100} \tag{3.3}$$

To prevent the system from the disturbance, feed forward transfer function must be as follows.

$$G_{ff} = -\frac{0.08469s^3 + 18.92s^2 + 796.8 + 36100}{680s + 35360} \tag{3.4}$$

This is a high pass filter but it is impossible to realize that. Because this transfer function does not represent a physical system. Also the derivative terms will bring to the system more oscillations while disturbance itself is oscillatory. Instead of this, a realizable high pass filter can be used which is constructed adding poles which are very high frequency for the system as in Figure 30 [17]. Adding poles to the system at -700 will be adequate because the bandwidth of the elevation axis model is approximately 200 rad/s.

$$G_{ff} = -\frac{0.08469s^3 + 18.92s^2 + 796.8 + 36100}{0.001388s^3 + 2.015s^2 + 781s + 35360} \tag{3.5}$$

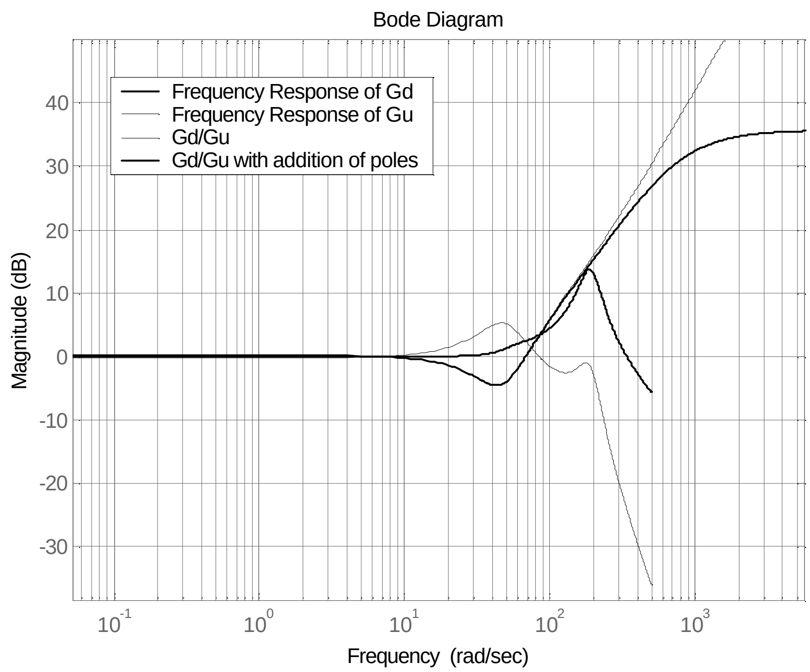

Figure 30. Bode Plot of the Disturbance Feed Forward Transfer Function

3.3. Feed Forward in Velocity Loops

Feed forward gains are used to speed up the response to rapidly changing position commands. Feed forward is often used in the cascaded position velocity loop. In this system, position loop enclose the velocity loop which is faster than itself. The feed forward path speeds response by-passing the slower position loop directly to the velocity loop (Figure 31).

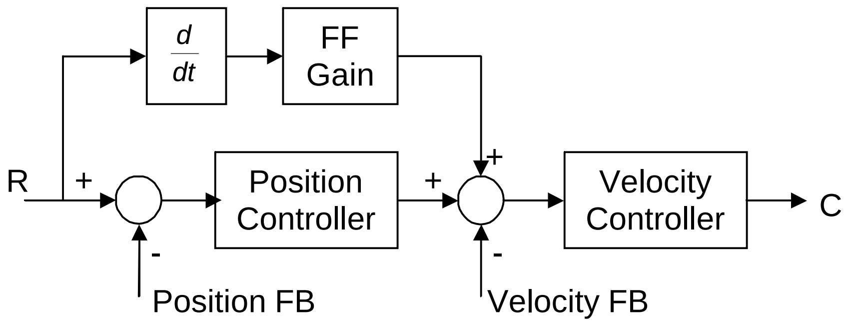

Figure 31. Velocity FF in Controller

In general, servo systems need high loop gains to have a good performance. High loop gain helps the controller to respond and reject disturbances. Since high servo gains may cause instability, they can be used limitedly. Thus feed forward can greatly improve the performance of a servo system.

The velocity feed forward path connects the velocity profile to the velocity loop through a gain. When the position profile abruptly changes, the velocity feed forward immediately passes that change to the velocity command. Velocity feed forward can reduce the time to make instant movement. But the disadvantage of this choice is produce overshoot. This can be settled by reducing the loop gains but to make this means also reduce the system disturbance rejection [18].

CHAPTER 4

SIMULATION

In this chapter, Simulink® models of the system components will be constructed and explained. Especially, servo valve identification and the friction model are handled in detail. Finally the complete system will be simulated for different cases. The simulations are made with a fixed time step of 5×10^{-4} s and the ODE5 (Dormand-Prince) solver is used. Because the fastest component of the system is the servo valve and its time constant is 0.0032 s. Since time step is very small, solution method also is selected 5^{th} order to be able to prevent the valuation error.

4.1. Valve Model and Identification Results

As explained in Chapter 2, the valve is separated into 2 parts. First part is made up of the linearized section which has the transfer function between the input voltage and the output valve's third stage spool position. Second part is the section where the flow is determined which maintains the nonlinearity of the orifices.

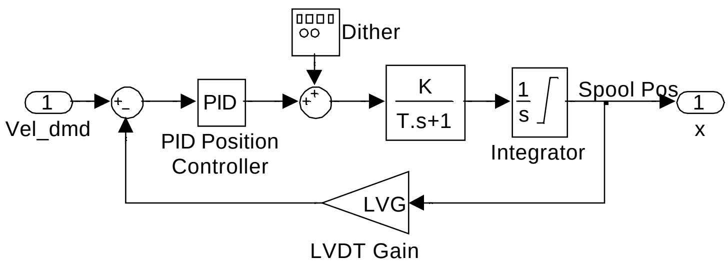

Figure 32. First Stage of the Servo Valve Model